International Journal of Structural Glass and Advanced Materials Research

Original Research Paper

A Novel Method for the Non-Destructive Assessment of Strength Degradation and Re-Use Potential of Weathered Float Glass From Facades: A Proof of Concept Study

[1]Fred Veer, [1]Mauro Overend, [2]Irene Sofokleous and [2]Chris Noteboom

[1]Faculty of Architecture and the Built Environment, Delft University of Technology, The Netherlands
[2]Faculty of Civil Engineering and Geosciences, Delft University of Technology, The Netherlands

Article history
Received: 26-06-2023
Revised: 14-09-2023
Accepted: 19-09-2023

Corresponding Author:
Fred Veer
Faculty of Architecture and the Built Environment, Delft University of Technology, The Netherlands
E-mail: f.a.veer@tudelft.nl

Abstract: Lack of knowledge about the properties of weathered (used) glass is currently a major barrier to glass reuse. This results in probably unnecessary recycling or down-cycling of architectural glass at the end of life. Avoiding this creates a significant opportunity to reduce resource depletion and decarbonize the built environment. This can be done by developing an optical non-destructive test method that estimates the strength of naturally weathered glass by characterizing surface flaws. This allows excessively damaged glass panels to be removed for surface repair or recycling. Specimens were made from 50^{+}-year-old monolithic flat glass taken from a façade in the Hague, Netherlands, where it was exposed to salt in the air, water, cleaning, and abrasion from wind-driven dust and sand particles. The specimens were examined using a microscope and a handheld optical profilometer to determine surface flaw characteristics. The glass specimens were then tested using a ring-on-ring (coaxial double ring) setup. Similar tests were also conducted on new as-received float glass to provide a benchmark. Both the indoor-facing and outdoor-facing sides of the weathered glass and the air and tin side of the new glass were tested. A statistical analysis of the test results was made using conventional Weibull statistics. The results show that after 50^{+} years of natural aging the strength of the glass is significantly reduced and that the non-destructive scanning method trialed in this study can locate and determine in many cases the size of critical surface defects thereby allowing for direct safe re-use of 70^{+}% of the glass. The handheld optical profilometer can identify severe damage on the glass, but further research and software development is needed to improve the accuracy and consistency of the scanning method and to automate this technique for routine/large-scale applications including as a prerequisite for surface repair.

Keywords: Weathering of Façade Glass, Strength of Weathered Glass, Glass Microscopy, Co-Axial Double Ring Testing, Glass Strength Statistics

Introduction

While glass is a very durable material, as testified by the many old windows in historical cities, the demand to reuse weathered glass in new buildings is relatively recent. Re-use has come to the fore recently because it would save considerably on the use of raw materials and energy and is thus highly desirable in the global quest to reduce eco-impact (Hartwell and Overend 2019; Hartwell *et al*., 2021). This is however currently limited by uncertainties about the strength of the old glass.

The degradation of window glass over time is commonly caused by weathering, a good summary of this phenomenon is given by Udi (2023). Weathering essentially has two components:

- Chemical corrosion of the glass
  - Leaching of Na^{+} ions from the glass by water
  - Breaking down of Si-O bonds by water under tension
- Mechanical abrasion of the glass
  - Pitting from impacts

DOI: 10.3844/sgamrsp.2023.1.15

- Scratches from abrasion of hard particles moving over the surface

The corrosion of the glass has been a problem since medieval times and is mostly determined by the chemistry of the glass (Newton, 1975). In modern float glass which is chemically much more stable, this is still a significant problem (Strugaj *et al*., 2021). So, most of the accumulated damage in weathered glass is from mechanical abrasion. The scratches and pits form stress concentrations which decrease the allowable stress before fracture occurs. Comparing the fracture surfaces of weathered and new glass has shown that the fracture mechanism in weathered and non-weathered glass is identical, (Reed and Bradt, 1984). Weathering thus reduces the strength by increasing the surface damage, but it does not change the physiochemistry of the fracture process.

Strength loss due to weathering can be determined by the co-axial double ring method, (Datsiou and Overend, 2017a-b) the vacuum technique (Abiassi, 1981; Sligar, 1989) or both (Dalgliesh and Taylor, 1990). The vacuum technique usually uses large specimens (entire windows) while the co-axial double ring method is used to determine the surface strength of smaller glass specimens (cut from windows). The vacuum technique essentially shows that the strength of complete windows degrades due to weathering. The co-axial double-ring test allows for a more detailed study of strength variation within a single weathered panel. Artificial aging using falling abrasive particles can be used to gain more insight into the mechanisms causing strength loss due to abrasion (Datsiou and Overend, 2017a-b).

All authors compared naturally weathered glass with factory-fresh new glass. All found a significant reduction in the mean strength of glass due to weathering. Typically, the mean strength of the weathered glass was about half the mean strength of new glass.

So, although it is well known that the strength of glass is reduced by weathering, all current regulations and building standards, such as ASTM E1300, FprCEN/TS 19100, NEN 2608:2014, do not differentiate between old and new glass. Practicing engineers are therefore reluctant to reuse existing glass because there is neither a generally accepted value for the strength of weathered glass nor any explicit guidelines on how to estimate the strength of such glass. As there are no non-destructive testing methods available, the only alternative is to undertake costly and time-consuming destructive experimental campaigns by testing specific batches of weathered glass on a case-by-case basis, which is unfeasible for most time and money-constrained real-world building projects.

However, as the strength of glass is generally governed by the condition of its surface, quantifying the defects on the surface allows for a non-destructive determination of the strength of weathered glass. Linear elastic fracture mechanics can be used to predict the strength with a high degree of accuracy, if the flaw size and shape are known. This follows the basic equation:

$$K_{Ic} = y\sigma_f\sqrt{(\pi a)}$$

With K_{IC} the fracture toughness, 0.55-0.7 MPa√m for glass, y a geometrical correction factor, σ_f the failure stress and the crack length. Essentially strength increases as defect size decreases. The size of the defect thus controls the engineering strength of annealed float glass.

If the fracture toughness and the geometrical correction factor are known, the failure stress can be calculated using measured crack length. This approach has been tested and verified by multiple authors (Holmes, 1997; Ai and Zhu, 2002: Overend and Zammit, 2012; Chen *et al*., 2015). This method is however not free from limitations as optical recognition of defects in glass depends a lot on the quality and number of reference images required to train the software (Agrawal, 2011). Also, the defects in glass tend to be irregular, and standard stress intensity factors cannot be used as these are based on defects in metals which tend to be regular and rounded. However, even if y is not known, a smaller defect size means stronger glass. Glass strong enough for reuse can thus be found if it can be determined that the defects are all below a critical size.

Identifying the location and size of critical surface flaws on glass is thus important for direct re-use, but it is also an essential prerequisite for the development of possible surface repair technologies. So, a good non-destructive flaw-finding inspection technology is critical for the future development of float glass re-use.

To summarise, the surface of the glass gets damaged by abrasion and corrosion. The resulting defects decrease the strength. If the size of critical defects is known, non-destructive optical testing of the surface can identify those weathered glass panels that cannot be re-used directly. Improvements in optical and software technology might provide the basis for such a testing method.

The objectives of this research project were therefore as follows:

- Find a supply of weathered glass
- Characterize the surface damage using an industrial optical profiler and a laboratory digital microscope
- Determine the surface strength of the weathered glass by destructive ring-on-ring tests
- Assess the correlation between the glass strength determined from destructive testing to the previously quantified surface damage
- Repeat the above on new glass to determine the relative loss of mean strength

DOI: 10.3844/sgamrsp.2023.1.15

Materials and Methods

Sourcing of the Glass and Its Chemical Composition

The weathered glass became available with the renovation of the office building at Koningskade 4 in The Hague, shown in Fig. 1. This building was designed in 1967 and built-in 1969 with a double skin façade. The outer skin was composed of large glass panels of 2.5×2.5 m of 10 mm thick monolithic float (soda lime silica) glass which were 50^{+} years old when they were carefully removed from the building in 2022 and taken away for storage. The location is 4 km from the sea and close to major roads. Pollution is thus more than average in the Hague region with the height of the building exposing the glass to higher wind and thus more abrasion. This could thus be considered a relatively severe exposure for a European location and therefore a reasonable worst-case example from the point of view of the research goals. A single panel was used to cut samples for this research. Two sample sizes, 250×250 and 450×450 mm, were used to compare side effects. The size was determined by the size of the available ring on ring testing equipment. At least 40 samples of each size were produced for both the weathered and the new glass. All specimens were cut by a commercial glazing firm using standard industrial glass cutting tables to ensure quality and consistency. Most of the glass was re-used to build IGUs for the Floriade natural pavilion.

The chemical composition of the glass panes used was determined by X-ray fluorescence. Both surfaces were tested after cleaning with demineralized water to remove surface residues that could potentially influence the measurements. The results are given in Table 1. Both the old and the new glass are well within the (ISO 16293-1, 2008) recommendations for soda lime silica float glass. No traces of tin were found on the surfaces of the old glass. This is not unusual for weathered float glass (Datsiou and Overend, 2016). The composition of both weathered and new glass is comparable although the former has a higher SO_3 and Cl content, suggesting that the production process was less clean than that used for the new glass. The differences however are too small to cause significant differences in physical properties. Therefore, on the basis of their chemical composition, it can be assumed that the glasses had nearly identical intrinsic (i.e., in their as-produced state) properties.

Surface Condition as Seen with a Digital Microscope

The cut samples were examined using a Keyence VHX 7000 digital microscope. Before examination, the examples were cleaned with a glass cleaning agent and soft tissue paper. It was easy to distinguish between inner and outer (exposed) surfaces. The differences are shown in Fig. 2. The presumed outer surface is characterized by more abrasion damage and clear corrosion damage. The presumed inner surface showed much less abrasion damage and corrosion damage. This difference was consistent for all specimens. Although surface damage was clearly visible with the digital microscope, it was not possible to quantify this damage in terms of defect depth with the lenses available. This also means that fracture mechanics calculations could not be made reliably as the crack shape and depth could not be determined in most cases.

Fig. 1: The office building at Koningskade 4 in the Hague from which the glass was sourced

Table 1: Chemical composition of tested glasses as found by XRF and according to ISO norm in wt. %

Chemical component	Old glass interior side	Old glass exterior side	New glass tin side	New glass air side	ISO 16293-1:2008
SiO_2	73.300	73.900	71.700	74.400	69-74
Na_2O	11.900	11.500	11.800	11.600	5-14
CaO	9.700	9.400	8.900	8.800	10-16
MgO	3.600	3.500	4.000	4.300	0-6
SnO_2	0.000	0.000	2.600	0.000	
Al_2O_3	0.400	0.600	0.490	0.530	0-3
K_2O	0.070	0.050	0.260	0.240	
Fe_2O_3	0.100	0.110	0.080	0.060	
SO_3	0.720	0.610	0.080	0.090	
Cl	0.074	0.050	0.020	0.020	
SrO	0.004	0.003	0.006	0.005	

DOI: 10.3844/sgamrsp.2023.1.15

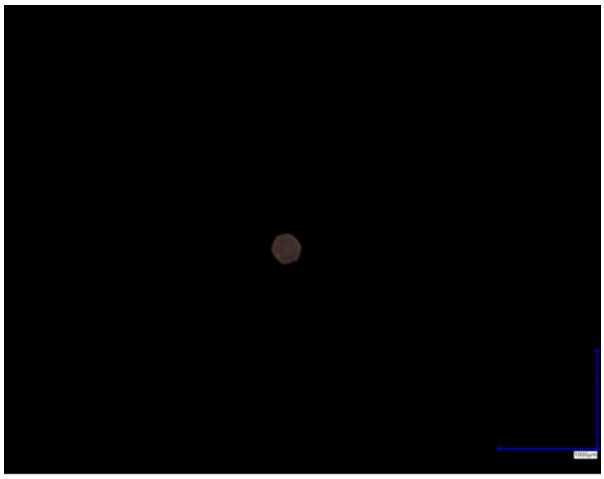

(a)

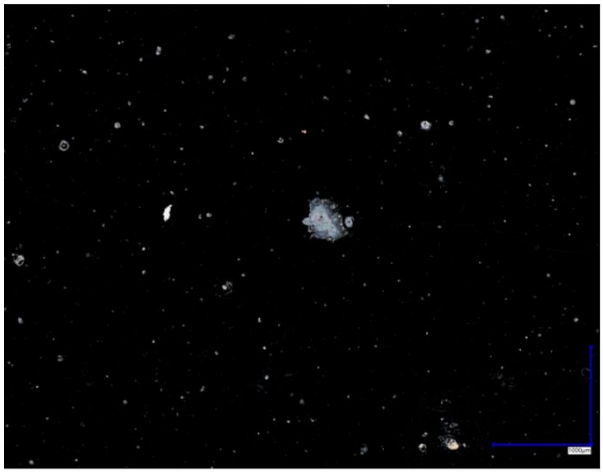

(b)

Fig. 2: Surface of weathered glass, left inner façade surface, right outer façade surface, magnification 200× (a) Surface presumed as inner; (b) Surface presumed as outer

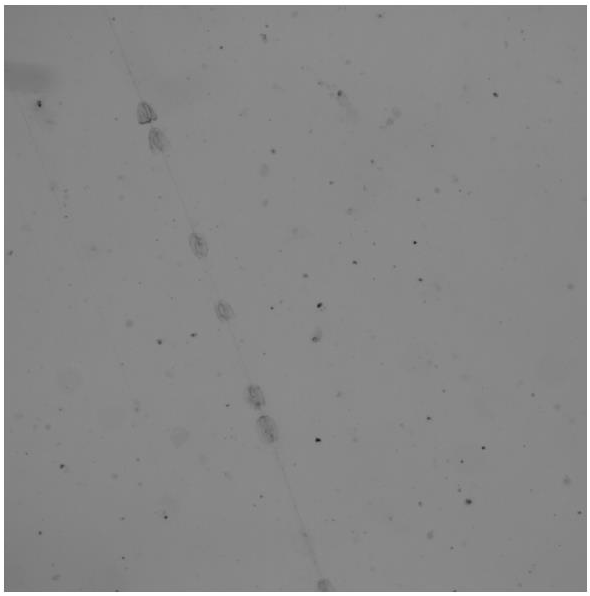

Fig. 3: TRACEiT image of weathered glass, left top lighting, right transmitted lighting

No observable difference was found between the two surfaces of the new glass, although the tin side could be determined easily with a standard UV tin detector.

Surface Condition as Measured with an Optical Profile Scanner

An optical profile scanner (TRACEiT manufactured by Innowep) was used in this study. It is an optical system that measures surface profiles by combining a lighting source, an optical camera, and software to make an accurate 3D assessment of a surface. The device was not specifically developed for scanning glass surfaces and no references could be found for using it on glass, so the settings had to be determined with support from the manufacturer and by trial and error, a full description is given in Sofokleous (2022). No physical changes were made to the scanner, only the software options were optimized for glass. The new glass specimens and the interior face of the weathered specimens showed no significant response to the optical profile scanner indicating that any defects present are smaller than the resolution of the scanner. Thus only the specimens with the weathered outside face in tension during the co-axial ring-on-ring test were fully scanned within the area of the loading ring. Figure 3 shows examples of images obtained from the optical profile scanner. The transmitted light image shows a linear scratch and localized damage zones along the scratch. To improve the image quality, the optical profile images were post-processed in PAINT.Net software or using MATLAB image processing algorithms. The results are shown in Fig. 4.

DOI: 10.3844/sgamrsp.2023.1.15

The system software of the optical profile scanner was used to determine the depth of defects based on the non-post-processed images, details are in Appendix C (Sofokleous, 2022). The post-processing thus only shows that major improvement in accuracy can be made, but the current scanner software does not allow for this. Large defects observed with the optical profilometer were marked on the glass with a marker pen prior to testing. The correlation between optical profile results and mechanical tests is discussed later in this study.

Mechanical Testing Method

Ring-on-ring (a.k.a. coaxial double ring) tests were conducted with ring dimensions selected in accordance with (ASTM C1499-09, 2013). The square glass specimens were placed in the ring-on-ring test jig mounted in a Zwick Z100 electro-mechanical testing machine operating with Zwick Testexpert III software. Two sets of rings were used: (i) A support ring of 150 mm diameter with a loading ring of 72 mm diameter for the smaller specimens and; (ii) A support ring of 250 mm diameter with a loading ring of 180 mm diameter. The size of the rings was based on the smallest set that could be used with this glass thickness and the largest stay that would allow tests within the loading range of the Zwick Z100. The set-up is shown in Fig. 5. Glass specimens were covered on both sides in transparent self-adhesive plastic foil to retain and examine the fragments after fracture. The jigs and glass specimens were carefully centered before each test and all tests were conducted at a constant displacement rate of 5 mm/min. This equates to a nominal stress rate of 7.6 MPa/s for the small specimens and 4.2 MPa/s for the large specimens.

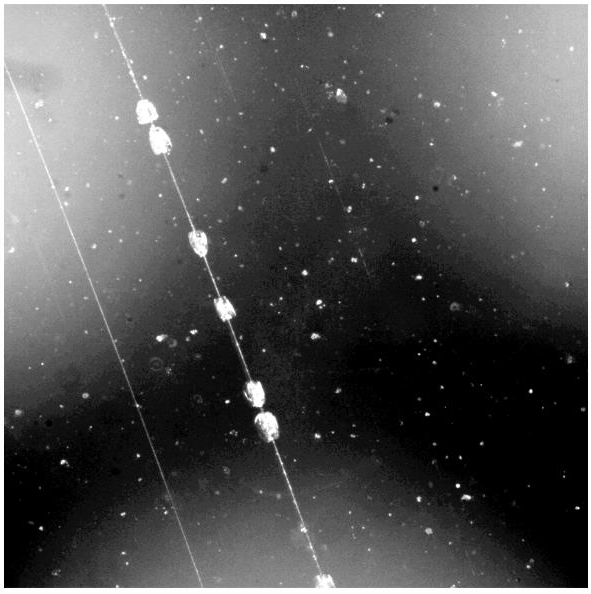

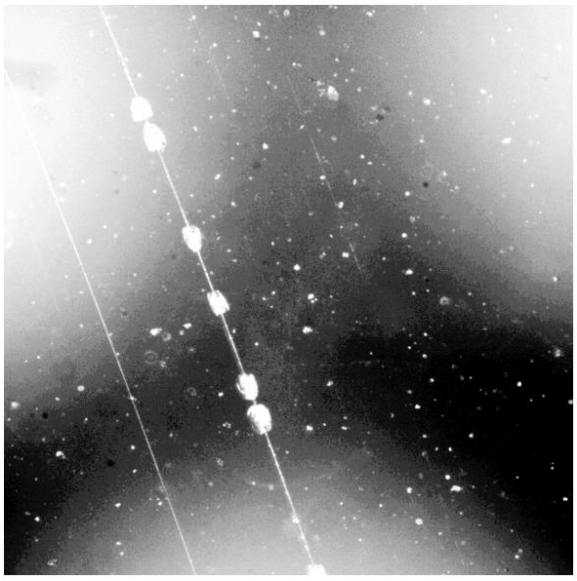

Fig. 4: Enhanced TRACEiT image using transmitted lighting after image processing, left with Paint.net software and right with Matlab histogram equalization

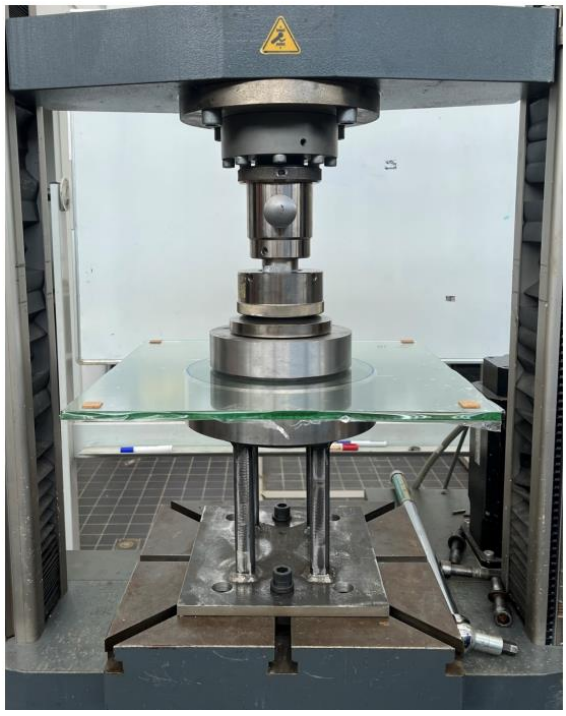

Fig. 5: Ring-on-ring set-up used for large specimens

This relatively high stress rate in combination with the self-adhesive plastic foil limits the effects of stress corrosion on the results. Load and displacement were registered using the Zwick Testexpert III software. Tests were conducted on two non-consecutive days, the first day for the weathered glass and the second day for the new

glass. The temperature on both days was between 20°C and 22°C and the relative humidity was between 50 and 55%, respectively. Higher humidity and temperature would increase the risk of stress corrosion of the glass and thus make comparative analysis more difficult.

Results

Experimental Results

There are 8 series of tests which are summarized in Table 2.

Test sets 1-4 provide data for weathered glass, the different sizes allow for the determination of a size effect. Test sets 5-8 provide data for new glass to show how much strength has been lost due to weathering.

The full results from these tests are shown in Appendix 1 and summarized in Table 3. Specimens with a fracture origin outside the loading ring area were deemed invalid and were not used in the subsequent analysis of the failure statistics as the failure stress could not be calculated. Furthermore, some of the small specimens with the air side in tension failed at very high stresses, which resulted in extensive fragmentation preventing the determination of the origin of failure, which means that the failure stress could not be calculated with certainty. These results were thus also not used in the statistical analysis as it was not certain the failure stress calculation was valid.

Correlation Between Defects Detected by Optical Profilometer and the Fracture Origin

In seven out of 21 of the small specimens, the fracture origin coincided with the location of a defect that had been identified by the optical profilometer and marked with a pen prior to testing. In the large specimens, the success rate was only 3 out of 22 specimens. As the glass had to be scanned manually, larger areas were more difficult to scan and it was difficult to mark all the surface damage.

Two examples of successful detection in small specimens are shown in Figs. 6-7. A 33% success rate is not particularly high, but these represent initial trials without specific tuning or optimization of the profilometer system for glass scanning. Figures 3-4 show, that the TRACEiT images require post-processing to make them clearer. As the TRACEiT software, which is not designed for use on glass, uses unprocessed images, the low success rate might be improved considerably by making small modifications to the image processing software, which however cannot be done by the user, only by the manufacturer.

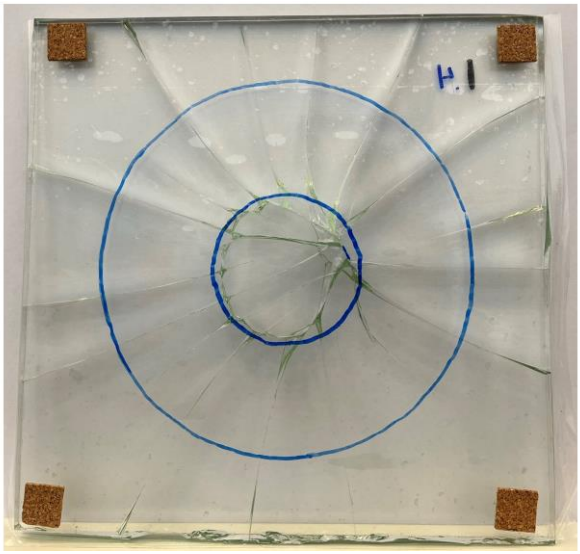

Fig. 6: Specimen after testing, critical defect successfully found by optical profilometer and marked before testing coinciding with the center of the butterfly crack pattern that is the start of the failure process

Table 2: Overview of tests conducted

Test set	Size (mm)	Number of tests	Number of tests with failure on or within loading ring	Surface in tension	Data
1	250×250	23	20	Weathered glass, interior surface	Appendix Table A1
2	250×250	21	16	Weathered glass, exterior surface	Appendix Table A2
3	450×450	24	24	Weathered glass, interior surface	Appendix Table A3
4	450×450	22	20	Weathered glass, exterior surface	Appendix Table A4
5	250×250	20	15	New glass, Sn side	Appendix Table A5
6	250×250	20	9	New glass, air side	Appendix Table A6
7	450×450	20	17	New glass, Sn side	Appendix Table A7
8	450×450	21	18	New glass, air side	Appendix Table A8

Table 3: Summary of results of ring-on-ring testing

	Mean σ_f (MPa)	Std σ_f (MPa)	Minimum σ_f (MPa)	Maximum σ_f (MPa)	Coefficient of variation
Small specimen, weathered glass, interior face in tension	104.1	20.7	60.3	138.2	0.199
Small specimen, weathered glass, exterior face in tension	63.6	15.7	37.1	88.9	0.247
A large specimen, weathered glass, interior face in tension	54.6	14.1	22.9	76.5	0.258
A large specimen, weathered glass, exterior face in tension	60.8	14.3	32.3	83.5	0.235
Small specimen, new glass, air side in tension	156.1	50.3	64.1	212.2	0.322
Small specimen, new glass, Tin side in tension	117.2	28.5	71.2	155.6	0.243
Large specimen, new glass, air side in tension	134.5	41.0	70.0	222.0	0.305
Large specimen, new glass, Tin side in tension	87.1	15.5	59.9	116.2	0.178

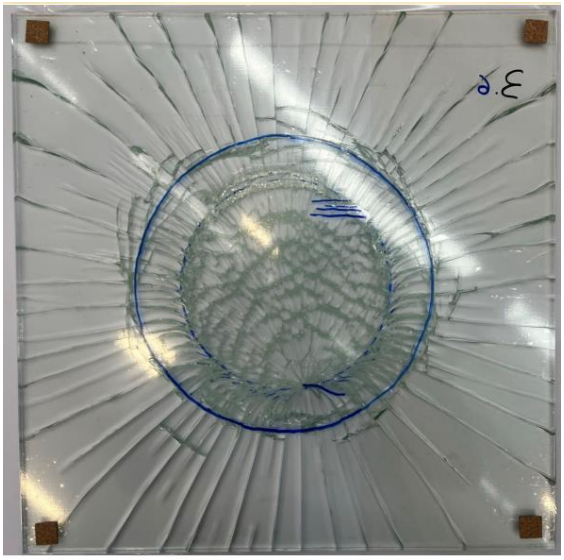

Fig. 7: Specimen after testing, critical defect successfully found by optical profilometer and marked before testing coinciding with the center of the butterfly crack pattern that is the start of the failure process

Discussion

The ultimate aim of this research is to establish whether the weathered glass is sufficiently strong for direct re-use. To answer this, the data from the ring-on-ring tests has been analyzed using Weibull plots in the MATLAB R2022a software. There is considerable discussion in the literature about the limitations of using Weibull distributions for glass failure statistics (Tumidajski, 2006; Kinsella and Persson, 2016; Iwuoha *et al*., 2023), many authors stated that the method is not reliable in determining the strength of materials. This does not affect the nature of the analysis made here which endeavours to understand the differences between distinct groups of data. So even if the Weibull method cannot determine the strength of glass accurately, the difference between the data sets is considered to be an indication of physical differences in the different test sets.

The data is summarized in Table 3. Important to note is that the coefficient of variation is very variable. The lowest strengths in each test series are between 30 and 50% of the highest strengths in each test set. The new glass shows as much variation as the old glass, if not more.

Figures 8-11 provide a direct comparison between the small specimen tests and the large specimen tests. Figure 8 reveals that there is no significant size effect for the weathered surface strength. Effectively the large and small specimens seem to form a single statistical group. This implies that the surface damage density is so high and relatively uniformly distributed across the whole surface that the probability of finding a critical defect is not significantly dependent on the size of the stressed area being tested.

Conversely, Fig. 9 shows that there is a significant size effect in the surface strength of the interior surface of the weathered glass. Here, larger specimens are significantly weaker than smaller specimens. The same can be observed for the new glass specimens with the Tin side in tension (Fig. 10). For these specimens apparently the defect density is much lower and more singular in nature, which means that a larger area has a greater probability of containing a critical defect.

DOI: 10.3844/sgamrsp.2023.1.15

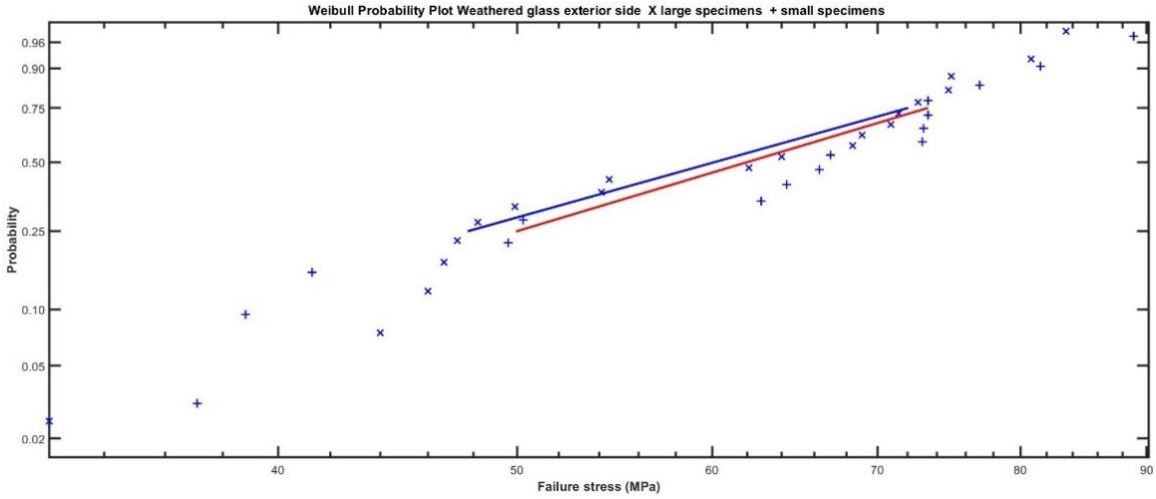

Fig. 8: Weibull plot of weathered specimens with exterior face in tension

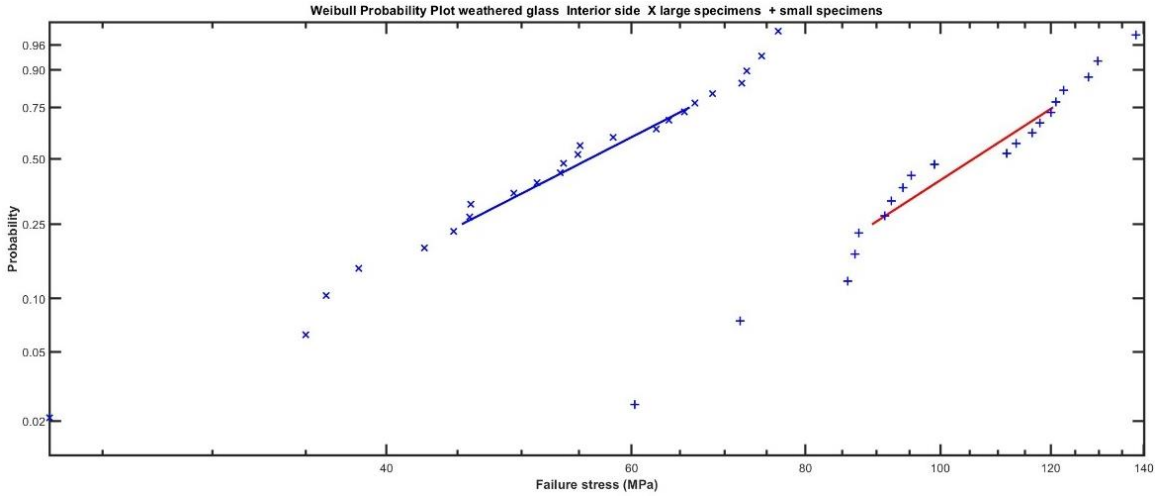

Fig. 9: Weibull plot of weathered specimens with the interior face in tension

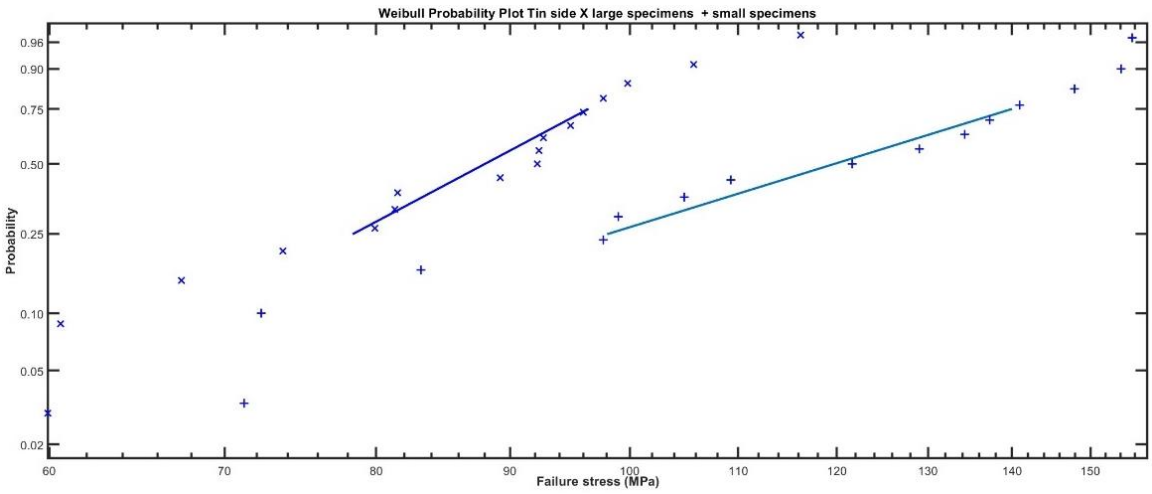

Fig. 10: Weibull plot of new glass, tin side in tension

DOI: 10.3844/sgamrsp.2023.1.15

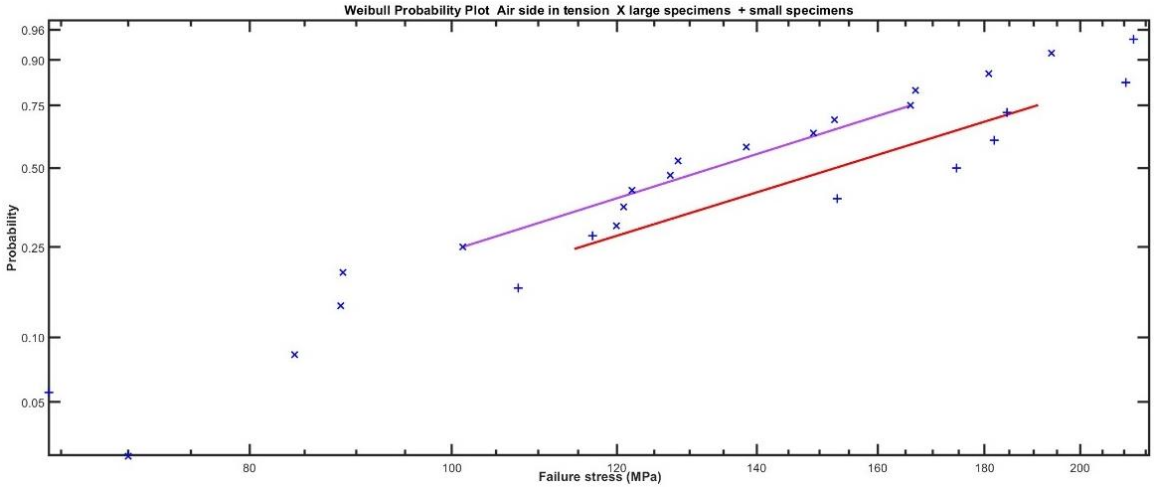

Fig. 11: Weibull plot of new glass, airside in tension

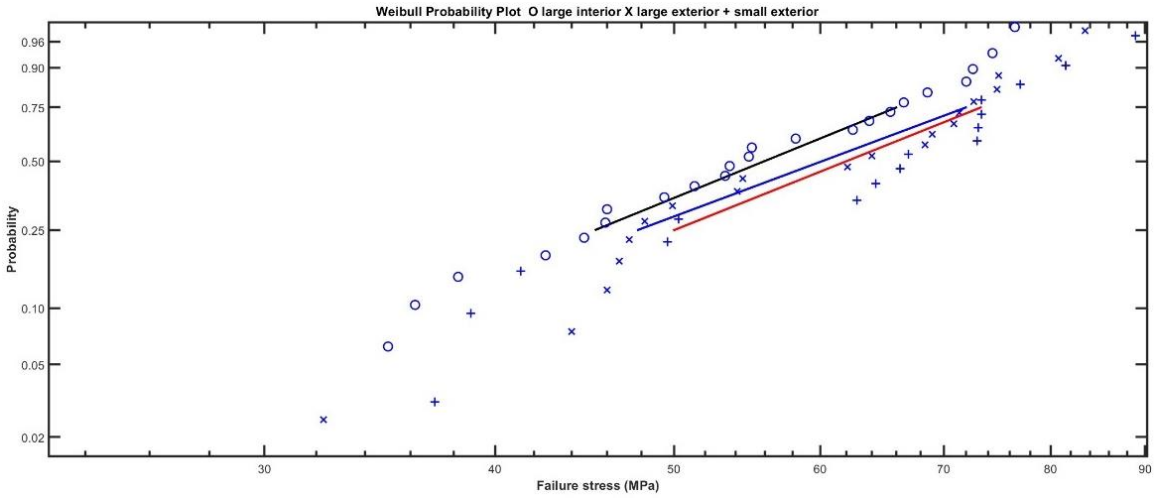

Fig. 12: Weibull plot of large interior, large exterior, and small exterior specimens

In what initially seems a paradox, the new glass specimens with the air side in tension, Fig. 11, have very little size dependency. However as the air side was not in contact with the rollers during the annealing phase of float glass production it is also the least damaged side, which is confirmed by the higher strength. A pristine glass surface should show no side effects. The new glass specimens with the air side in tension thus approximate such an "undamaged" surface.

The Weibull plots of the large interior, large exterior, and small exterior weathered glass specimens in a single graph (Fig. 12) show a reasonable coincidence, except for the lower outlier of the large interior data set. This would suggest that large surfaces of weathered glass both interior and exterior, excepting the occasional outlier, converge to a minimum strength of around 30 MPa. For a probability of failure of 2-5%. It should be noted that due to the limited number of data points, this cannot be calculated exactly. This implies that if outliers can be removed by a non-destructive evaluation method, using for instance an improved TRACiT scanner system, the residual glass should have a safe design strength of around 30 MPa. In statistical terms, this is in effect a left-truncated distribution or a bi-modal distribution as reported (Ballarini *et al*., 2016; Datsiou and Overend, 2018), respectively. Since the glass has been weathered for 50^+ years and the distributions of the large interior and large and small exterior specimens seem to coincide in a Weibull plot, this implies that the weathering damage has reached a limit, in this particular location and use-case, during the 50^+ years of exposure to weathering, cleaning etc. The outliers could potentially be explained by singular phenomena such as either a pre-existing defect or a defect produced by something other

than weathering, for instance, a bird impact or damage induced during transportation or cleaning. In other words, outliers might be part of a different statistical population and not representative of damage due to normal weathering.

An important point is that the optical profilometer was successful in several cases in finding the defect that would lead to failure as Figs. 6-7 show. The low success rate is probably due to the fact that the scanner software does not post-process the images before calculating flaw depth. Figs. 3-4 shows that post-processing results in much more contrast, it is likely that the detection rate can be improved significantly by improved software.

Conclusion

From the results, the authors conclude that:

- There is an approximately 50% reduction in the mean strength of window glass due to weathering compared to new glass. This decrease in strength is comparable to that found in the literature which suggests that these results are generally applicable and that weathering of glass, except for the occasional statistical outlier, leads to a maximum 50% reduction in glass strength The optical profiler can in many cases find the critical surface defect non-destructively using current software
- Post-processing of optical profiler images makes the flaws much more visible and seems to offer the potential to increase the accuracy considerably but requires improvements to the software and perhaps to the hardware to provide more calculating power
- The strength data distributions coincide for large specimens with the interior face in tension and large and small specimens with the exterior face in tension
- This suggests that the weathering process has reached a maximum damage level for this weathered glass after 50^{+} years and that further weathering would not result in larger flaws
- Excepting outliers caused by singular events and not by weathering, this implies a minimum strength of approximately 30 MPa for weathered glass at a probability of failure of 2-5%. Thus most weathered glass should be safe for re-use as the 30 MPa is strong enough for regular use in windows
- The air side of new glass is on average 40-50% stronger than the tin side of new glass
- The results from the initial study described in this study are sufficiently promising to warrant further work, in particular
- conduct more tests using a broad range of glass thicknesses, glass treatments (coated, heat treated, etc.,) and glass from different locations to create a comprehensive database on weathered glass strength
- make the software and hardware adjustments required to improve the flaw-detection capabilities of the optical scanning technology
- For the microscope try to use lenses with higher magnification for 3D image flaws
- explore ways of identifying glass surface damage too big to allow direct re-use and using chemical or thermal techniques to remove this damage

Acknowledgment

The authors would like to acknowledge the following firms and people for their help in this research:

- Innowep GmbH for providing the Traceit® scanner and instructing us in the use of it
- Scheldebouw B.V. for providing the weathered glass
- Hermans Groep for the processing and transportation of the weathered glass specimens
- ABT and Versteeg Zichtbaar in Glas for providing the specimens of new glass
- Ruud Hendrikx, TU Delft, for doing the XRF measurements
- Prof. Christian Louter and Erwin ten Brincke for their suggestions and help in doing the research

Funding Information

The research was conducted as an MSc graduation project at TU Delft. No direct funding was provided although the material was supplied without cost and processing and transportation costs paid for by industry. Other costs were paid for by TU Delft.

Author's Contributions

Fred Veer: Supervised the experiments, analysed the data, wrote the paper.

Mauro Overend: Headed the research and provided critical expertise on experimental techniques. Provided critical feedback on the paper.

Irene Sofokleous: Did the experiments, analysed the data provided feedback on the paper.

C. Noteboom: Provided valuable expertise from practice, arranged test materials provided feedback on the paper.

Ethics

There are no ethical considerations besides the research aim of obtaining a significant reduction in energy and material consumption in the built environment.

Conflict of Interest

The authors confirm there is no conflict of interest.

References

Abiassi, J. J., (1981). The strength of weathered window glass using surface characteristics, MSc thesis university of Texas. https://ttu-ir.tdl.org/handle/2346/61306

Agrawal, S. (2011). Glass defect detection techniques using digital image processing-a review. IP Multimedia Communications, 65-67.

Ai, J., & Zhu, X. (2002). Analysis and detection of ceramic-glass surface defects based on computer vision. *Proceedings of the 4th World Congress on Intelligent Control and Automation* (*Cat. No.02EX527)*, *4*, 3014-3018. https://doi.org/10.1109/WCICA.2002.1020081

ASTM C1499-09. (2013). Standard test method for monotonic equibiaxial flexural strength of advanced ceramics at ambient temperature. https://www.astm.org/c1499-19.html

Ballarini, R. Pisano, G. & Royer-Carfagni, G. (2016) The Lower Bound for Glass Strength and Its Interpretation with Generalized Weibull Statistics for Structural Applications. *Journal of Engineering Mechanics*, *142*(12), 2016. https://doi.org/10.1061/(ASCE)EM.1943-7889.0001151

Chen, Z., Shen, Y., Bao, W., Li, P., Wang, X., & Ding, Z. (2015). Identification of surface defects on glass by parallel spectral domain optical coherence tomography. *Optics Express*, *23*(18), 23634. https://doi.org/10.1364/OE.23.023634

Kinsella, D. T., & Persson, K. (2016, June). On the applicability of the Weibull distribution to model annealed glass strength and future research needs. In *Challenging Glass Conference Proceedings* (Vol. *5*, pp. 593-608). https://doi.org/10.7480/cgc.5.2432

Dalgliesh, W. A., & Taylor, D. A. (1990). The strength and testing of window glass. *Canadian Journal of Civil Engineering*, *17*(5), 752-762. https://doi.org/10.1139/l90-088

Datsiou, K. C., & Overend, M. (2016). Evaluation of artificial ageing methods for glass. *Challenging Glass Conference Proceedings*, *5*: 581-592. https://doi.org/10.7480/cgc.5.2431

Datsiou, K. C., & Overend, M. (2017a). The strength of aged glass. *Glass Structures and Engineering*, *2*, 105-120.
https://doi.org/10.1007/s40940-017-0045-6

Datsiou, K. C., & Overend, M. (2017b). Artificial ageing of glass with sand abrasion. *Construction and Building Materials*, *142*, 536-551. https://doi.org/10.1016/j.conbuildmat.2017.03.094

Datsiou, K. C., & Overend, M. (2018). Weibull parameter estimation and goodness-of-fit for glass strength data. *Structural Safety*, *73*, 29-41. https://doi.org/10.1016/j.strusafe.2018.02.002

Hartwell, R. Macmillan, S., & Overend, M., (2021) Circular economy of facades: Real world challenges and opportunities, Resources, *Conservation and Recycling*, *175*, 2021. https://doi.org/10.1016/j.resconrec.2021.105827

Hartwell, R., & Overend, M. (2019). Unlocking the re-use potential of glass Façade systems. *Glass Performance Days*, *2019*, 273-280.

Holmes, J. D. (1997, July). Inspection of float glass using a novel retroreflective laser scanning system. In *Optical Scanning Systems: Design and Applications* (Vol. 3131, pp. 180-190). SPIE. https://doi.org/10.1117/12.277748

ISO 16293-1. (2008). Glass in building - Basic soda lime silicate glass products-Part 1: Definitions and general physical and mechanical properties.

Iwuoha, S. E., Seim. W, & Olaniran. S. O. (2023). Statistical distributions and their influence on the material property values of tropical timber Case study of Gmelina arborea, Structures, 2023, in press. https://doi.org/10.1016/j.istruc.2023.04.059

Newton, R, (1975). The weathering of medieval window glass, *Journal of Glass Studies*, *17*, p 161-169, 1975. Optical Scanning Systems: *Design and Applications*, *3131*, 180-190. https://doi.org/10.1117/12.277748

Overend, M, K. & Zammit, (2012). A computer algorithm for determining the tensile strength of float glass, *Engineering Structures*, Volume *45*, December 2012, Pages 68-77. https://doi.org/10.1016/j.engstruct.2012.05.039

Reed, D. A., & Bradt, R. C. (1984). Fracture Mirror-Failure Stress Relations in Weathered and Unweathered Window Glass Panels, *Communications of the American Ceramic Society*, *C 227*, November 1984. https://doi.org/10.1111/j.1151-2916.1984.tb19490.x

Sligar, J. W., (1989). Evaluation of weathered window glass strength, MSc thesis university of Texas, 1989.

Sofokleous, I. (2022). Methodology for the prediction of the strength of naturally aged glass based on surface flaw characterization, *MSc thesis Delft University of Technology* 2022.

Strugaj, G. Herrmann, A., & Radlein, E. (2021). AES and EDX surface analysis of weathered float glass exposed in different environmental conditions. *Journal of Non-Crystalline Solids*, *vol 572*, 2021. https://doi.org/10.1016/j.jnoncrysol.2021.121083

Tumidajski, P. J., Fiore L., Khodabocus, T., Lachemi M., & Pari R., (2006) Comparison of Weibull and 375 normal distributions for concrete compressive strengths, *Can. J. Civ. Eng*. *33* (2006), 1287-1292. https://doi.org/10.1139/l06-080

Udi, U. J., Yussof, M. M., Ayagi, K. M., Bedon, C., & Kamarudin, M. K. (2023). Environmental degradation of structural glass systems: A review of experimental research and main influencing parameters. *Ain Shams Engineering Journal*, *14*(5), 101970. https://doi.org/10.1016/j.asej.2022.101970

Appendix 1: Results

Table A1: Test results for weathered glass, interior face in tension, 250×250 mm size

Specimen number	F_f (N)	σ_f (MPa)	Failure inside or on loading ring
1	10850	71.800	Yes
3	9159	60.300	Yes
4	17776	117.900	Yes
5	13111	87.400	Yes
6	19147	127.700	Yes
7	18142	120.000	Yes
8	14943	99.000	Yes
9	13859	92.200	Yes
10	20620	138.200	Yes
11	17092	113.300	Yes
12	18309	122.600	Yes
13	14113	94.000	Yes
14	19453	129.800	Yes
15	17548	116.400	Yes
18	12996	86.800	Yes
19	14261	95.300	Yes
20	12738	85.800	Yes
21	16662	111.600	Yes
22	18046	121.000	Yes
23	13624	91.200	Yes
	Number of valid tests	20 = 87%	
	Mean of valid tests	104.100	
	Coefficient of variation of valid tests	0.199	
2	8099	54.100	No
16	14030	93.800	No
17	15103	101.200	No

Table A2: Test results for weathered glass, exterior face in tension, 250×250 mm size

Specimen number	F_f (N)	σ_f (MPa)	Failure inside or on ring
1	9925	67.000	Yes
2	13299	88.900	Yes
4	5731	38.800	Yes
5	11987	81.500	Yes
7	10887	73.400	Yes
9	7419	49.600	Yes
10	10903	73.100	Yes
11	9956	66.300	Yes
12	9590	64.300	Yes
13	11457	77.000	Yes
14	6165	41.300	Yes
15	10849	73.000	Yes
16	10945	73.400	Yes
17	7481	50.300	Yes
18	5475	37.100	Yes
21	9455	62.800	Yes
	Number of valid tests	16 = 76%	
	Mean of valid tests	63.600	
	Coefficient of variation of valid tests	0.2470	
3	12502	83.300	No
6	13078	88.100	No
8	8679	58.400	No
19	10478	71.100	No
20	10513	70.800	No

DOI: 10.3844/sgamrsp.2023.1.15

Table A3: Test results for weathered glass, internal face in tension, 450×450 mm size

Specimen number	F_f (N)	σ_f (MPa)	Failure inside or on ring
1	25548	62.5000	Yes
2	30460	74.4000	Yes
3	31287	76.5000	Yes
4	18329	44.7000	Yes
5	29705	72.6000	Yes
6	27295	66.6000	Yes
7	26854	65.5000	Yes
8	22037	53.6000	Yes
9	9606	22.9000	Yes
10	22514	54.9000	Yes
11	21148	49.4000	Yes
12	19160	46.0000	Yes
13	21581	51.3000	Yes
14	15412	36.2000	Yes
15	17846	42.6000	Yes
16	15773	38.2000	Yes
17	24322	58.2000	Yes
18	28827	68.6000	Yes
19	19468	45.9000	Yes
20	23096	55.1000	Yes
21	26743	63.8000	Yes
22	22255	53.30000	Yes
23	14670	35.0000	Yes
24	30023	72.0000	Yes
	Number of valid tests	24 = 100%	
	Mean of valid tests	54.6000	
	Coefficient of variation of valid tests	0.2580	

Table A4: Test results for weathered glass, external face in tension, 450×450 mm size

Specimen number	F_f (N)	σ_f (MPa)	Failure inside or on ring
1	29505	71.400	Yes
2	33856	80.800	Yes
3	20645	49.900	Yes
4	22433	54.100	Yes
5	25523	62.100	Yes
6	30821	75.000	Yes
7	26313	64.000	Yes
8	22502	54.500	Yes
9	29529	70.900	Yes
11	13417	32.300	Yes
12	34905	83.500	Yes
13	20146	48.200	Yes
14	19478	46.700	Yes
15	30612	72.700	Yes
16	19923	47.300	Yes
17	18456	44.000	Yes
18	19269	46.000	Yes
19	28549	68.400	Yes
20	31102	74.800	Yes
22	28842	69.000	Yes
	Number of valid tests	20 = 90.9%	
	Mean of valid tests	60.800	
	Coefficient of variation of valid tests	0.235	
10	28661	69.300	No
21	17224	41.400	No

DOI: 10.3844/sgamrsp.2023.1.15

Table A5: Test results for new glass, Tin side in tension, 250×250 mm size

Specimen number	F_f (N)	σ_f (MPa)	Failure inside or on ring
1	15479	97.700	Yes
2	21389	134.300	Yes
3	11567	71.200	Yes
4	17903	109.300	Yes
5	16803	104.900	Yes
6	20474	129.000	Yes
7	24817	155.600	Yes
9	25365	154.100	Yes
10	21908	137.300	Yes
11	19404	121.600	Yes
12	15910	99.000	Yes
13	13600	83.200	Yes
15	11677	72.300	Yes
19	22821	140.900	Yes
20	23320	147.900	Yes
	Number of valid tests	15 = 75%	
	Mean of valid tests	117.200	
	Coefficient of variation of valid tests	0.243	
8	16584	102.600	No
14	9330	57.900	No
16	16682	104.400	No
17	17225	106.800	No
18	9482	59.100	No

Table A6: Test results for new glass, air side in tension, 250×250 mm size

Specimen number	F_f (N)	σ_f (MPa)	Failure inside or on ring
1	30090	184.500	Yes
2	34332	210.300	Yes
4	28144	174.500	Yes
6	19081	116.800	Yes
10	24983	153.000	Yes
11	10294	64.100	Yes
16	17375	107.600	Yes
19	29804	182.000	Yes
20	34430	212.200	Yes
	Number of valid tests	9 = 45%	
	Mean of valid tests	156.100	
	Coefficient of variation of valid tests	0.322	
3	36960	229.900	Could not be determined due to extreme fragmentation
5	33881	207.100	No
7	37109	227.500	No
8	32884	206.600	No
9	30906	189.100	No
12	45910	282.400	Could not be determined due to extreme fragmentation
13	47827	292.100	Could not be determined due to extreme fragmentation
14	27080	167.400	Could not be determined due to extreme fragmentation
15	25047	157.400	No
17	35233	218.500	Could not be determined due to extreme fragmentation
18	30047	187.400	Could not be determined due to extreme fragmentation

DOI: 10.3844/sgamrsp.2023.1.15

Table A7: Test results for new glass, Tin side in tension, 450×450 mm size

Specimen number	F_f (N)	σ_f (MPa)	Failure inside or on ring
1	27541	60.600	Yes
2	44858	99.800	Yes
3	42683	92.700	Yes
4	41130	89.200	Yes
5	43465	94.900	Yes
7	42676	92.200	Yes
8	37667	81.300	Yes
10	44519	96.000	Yes
11	47597	105.800	Yes
12	35863	79.900	Yes
13	27620	59.900	Yes
14	31014	67.400	Yes
15	33834	73.700	Yes
16	42957	92.300	Yes
17	36872	81.500	Yes
18	44075	97.700	Yes
19	52219	116.200	Yes
	Number of valid tests	17 = 85%	
	Mean of valid tests	87.100	
	Coefficient of variation of valid tests	0.178	
6	28787	62.500	No
9	17654	38.300	No
20	37813	84.400	No

Table A8: Test results for new glass, Air side in tension, 450×450 mm size

Specimen number	F_f (N)	σ_f (MPa)	Failure inside or on ring
1	74533	166.800	Yes
3	39485	88.700	Yes
4	86864	193.800	Yes
5	54742	122.000	Yes
6	69150	152.500	Yes
7	54227	120.900	Yes
8	100000	222.000	Yes
10	46430	101.200	Yes
11	55872	119.900	Yes
12	59315	127.300	Yes
13	76943	165.900	Yes
14	64453	138.400	Yes
15	40864	88.500	Yes
16	68611	149.000	Yes
17	38661	84.100	Yes
18	81383	180.800	Yes
20	32343	70.000	Yes
21	58782	128.4000	Yes
	Number of valid tests	18 = 85.7%	
	Mean of valid tests	134.500	
	Coefficient of variation of valid tests	0.305	
2	61124	136.900	No
9	83163	185.800	No
19	48089	103.600	No